Electron Microscopy: 3D reconstruction and validation

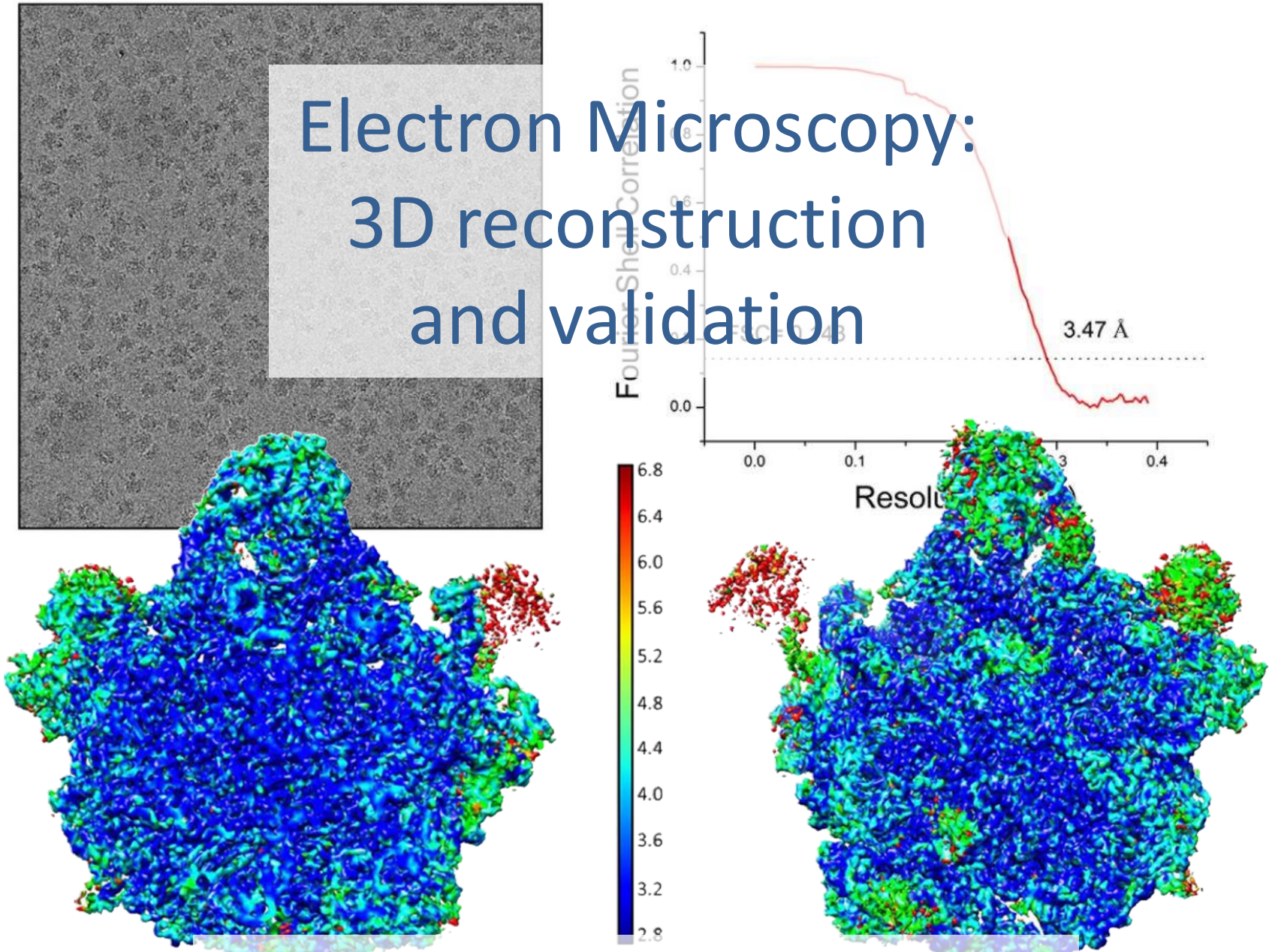

Corso di Biocristallografia e Microscopia Elettronica

rdezorzi@units.it

3D reconstruction

Reconstruction is the process to obtain from 2D images of particles the 3D map of electrostatic potential (volume of the object)

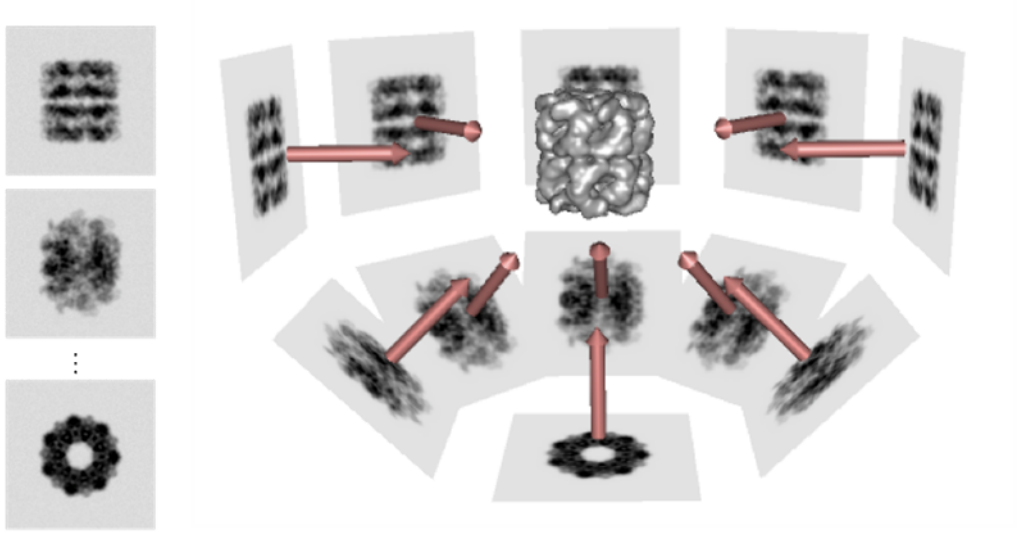

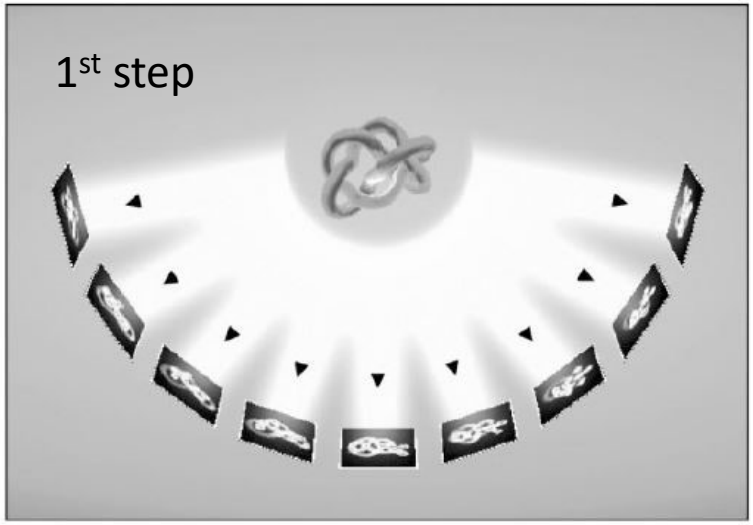

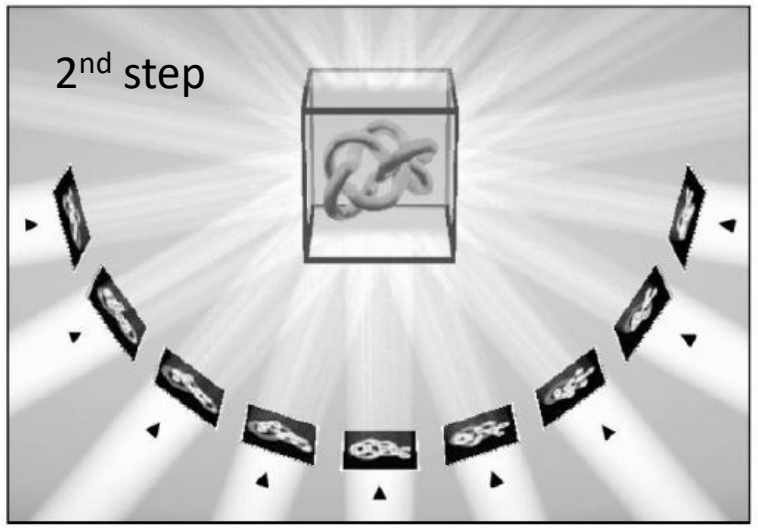

The reconstruction is carried on in 2 steps:

1. Determination of the Euler angles of each particle image
2. Reconstruction of the volume from the images with assigned angles

Some basic ideas…

Euler angles:

Rotation angles of each particle compared to the incident electron beam, determining the projection of particles in a different orientation

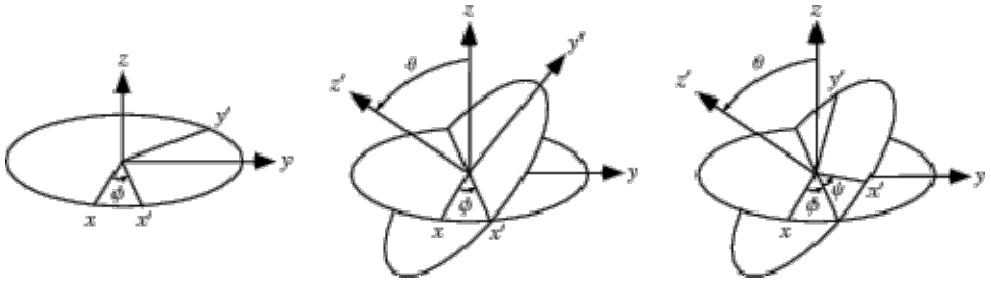

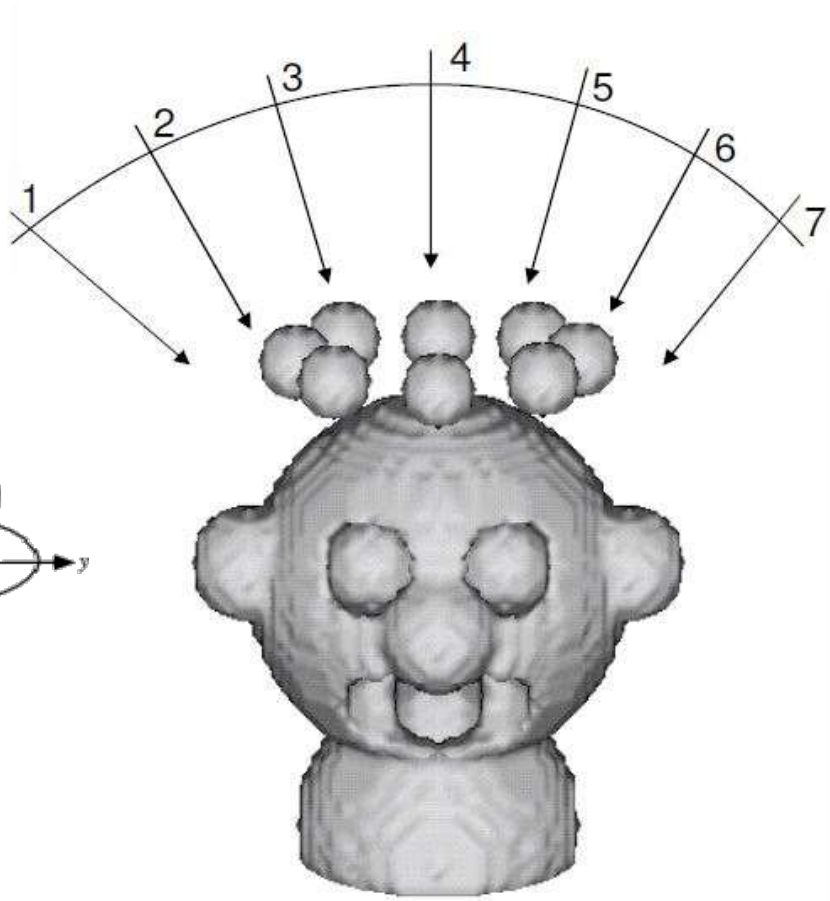

Projection:

The image of the particle obtained from the micrographs is NOT just the shape of the molecule, but the **projection of the electrostatic potential** of the protein: features are present in the interior of particles.

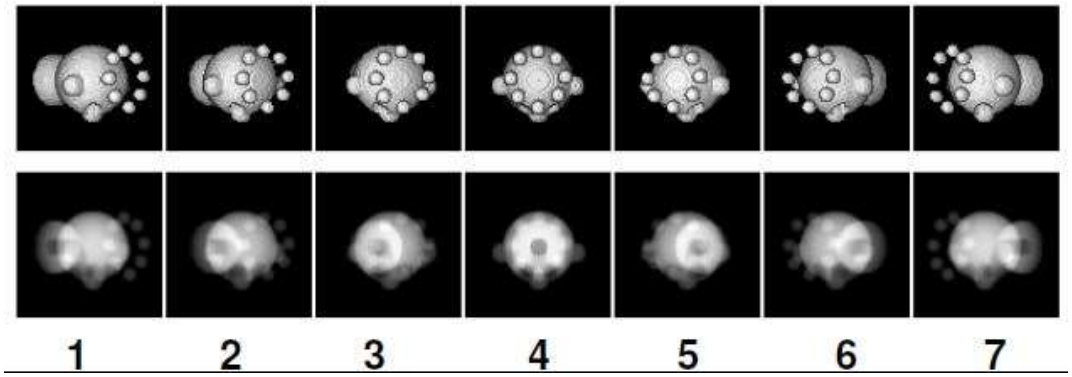

Step 1: Euler angles determination

For reconstruction, projections of the particles in different orientations are required.

To each particle orientation (Euler angles) must be assigned.

1

Reconstruction from many images of the same particle in different orientations:

ELECTRON TOMOGRAPHY

Relative orientation of images is known from the experiment: tilt angle

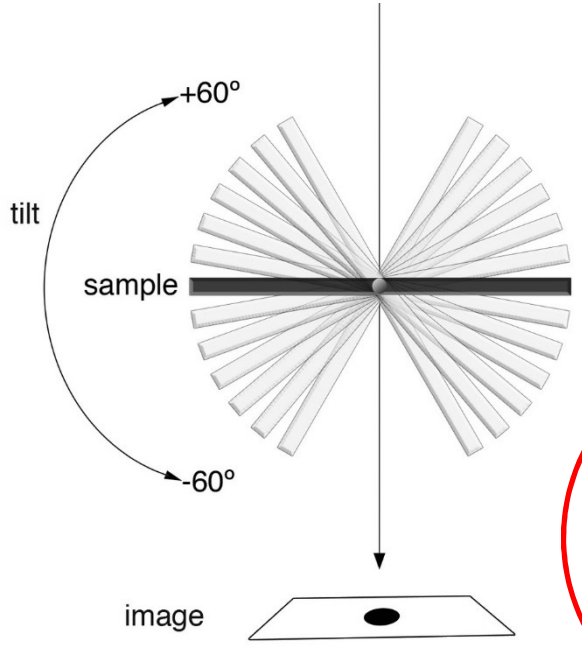

Low resolution due to radiation damage

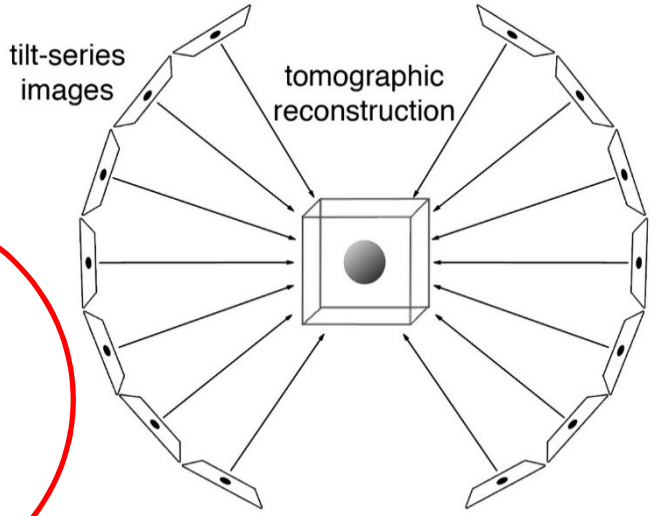

2 Random Conical Tilt Method

For grids with preferential orientation
(e.g. negative staining)
Collection of ‘tilt pairs’ – 45° and 0° tilt

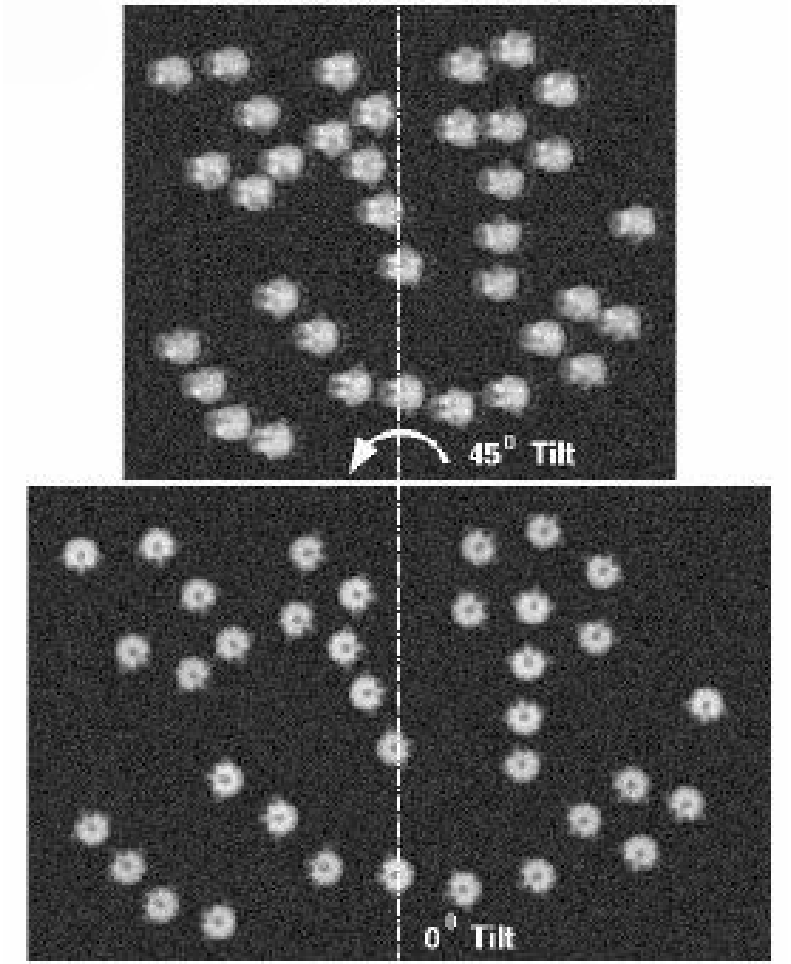

Particles selected from tilt pairs **Euler angles** are known from the tilt axis&angle

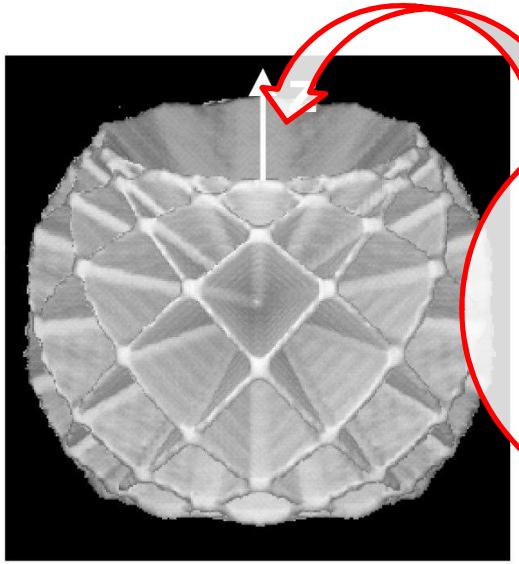

Missing cone can cause distortions in the structure

1. Data collection: collect a 45°-tilted image
2. Data collection: on the same grid position, collect untilted image

   0°-tilt images will not be used for final 3D reconstruction, but only for identification of Euler angles.

3. Interactive windowing of particles in the two micrographs. Centering and masking.

   At 0° tilt, projections of the same object are identical except for in-plane rotation (Euler angle φ). At 45°, particles are different.

4. Alignment and classification of particles from 0°-tilt to identify φ_i.

   Other Euler angles identified from tilt geometry. Determination of correct tilt geometry is crucial!

5. Scaling of tilted data.

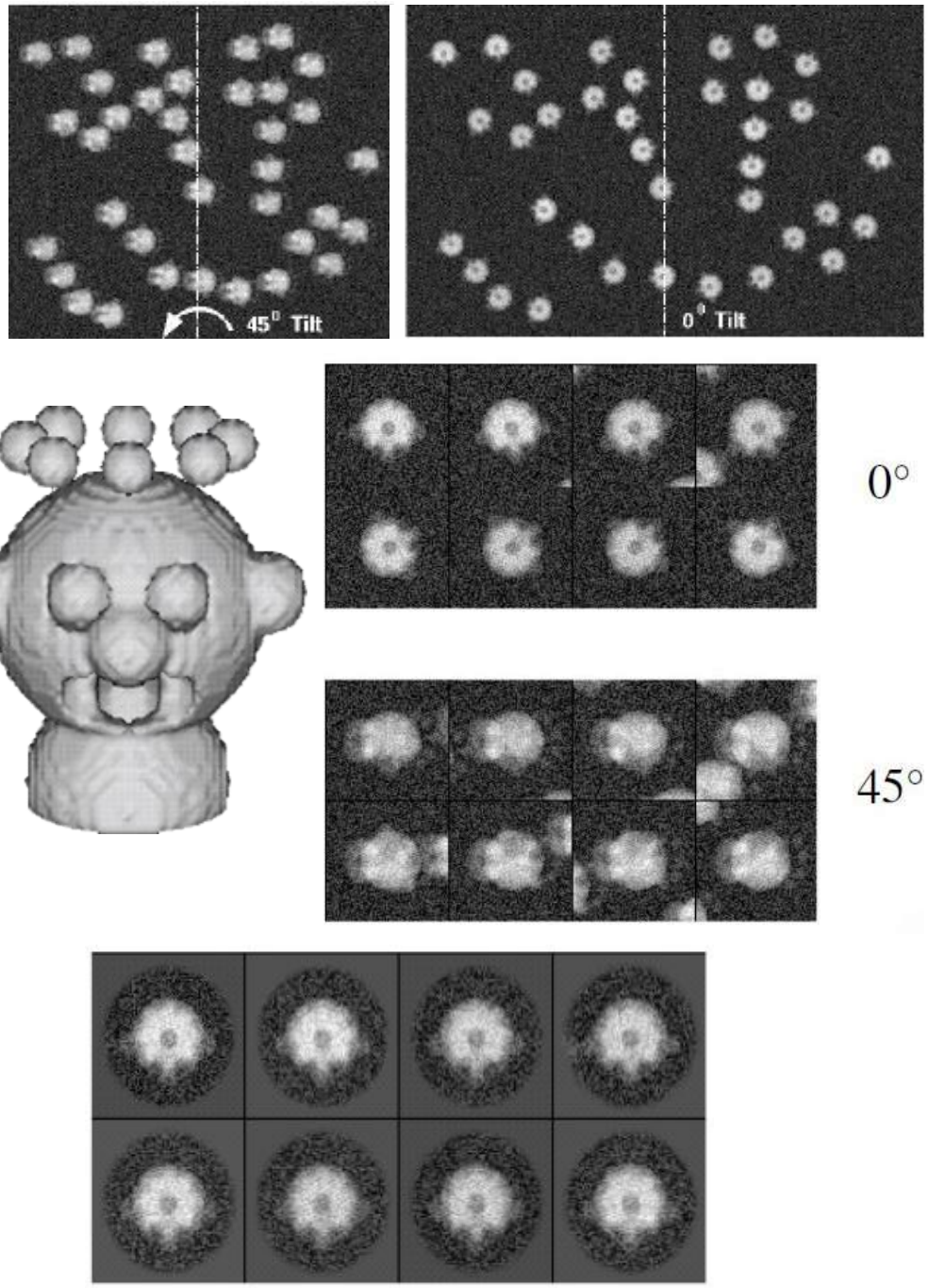

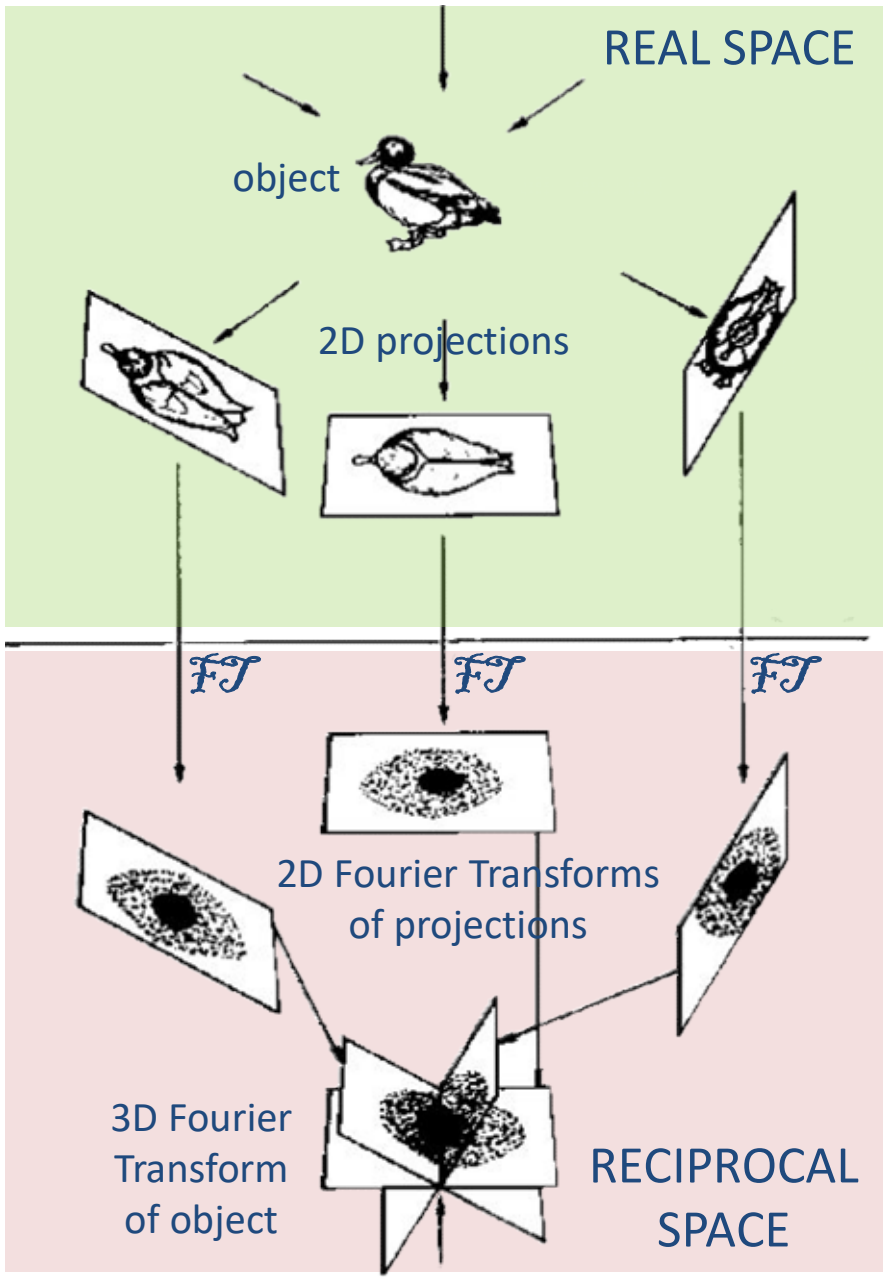

Projection Theorem (or Radon's Theorem)

In reciprocal space, every 2D projection of a 3D object corresponds to a 2D central section of the 3D Fourier transform of the object.

The central section obtained from the Fourier transform of a projection is orthogonal to the direction of the projection.

Considering this theorem, the reconstruction of the object from 2D projections is possible, but…

(1) How many images are required? What is the necessary coverage of the reciprocal space?

(2) Would reconstruction be unique?

3 Common-Lines Method

If images of particles are collected in random orientations (e.g. cryo-EM):

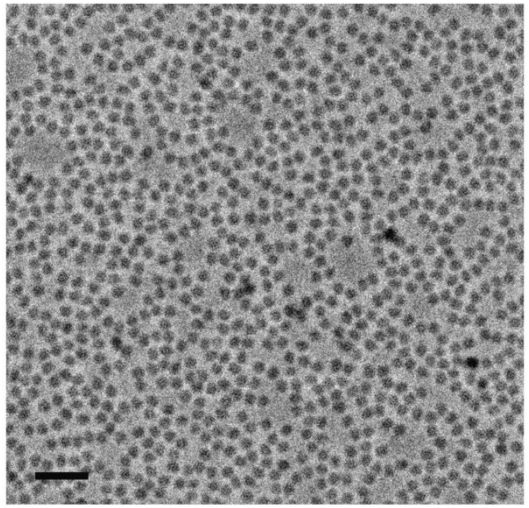

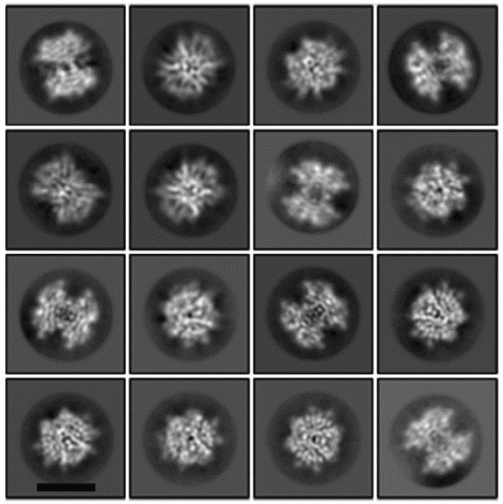

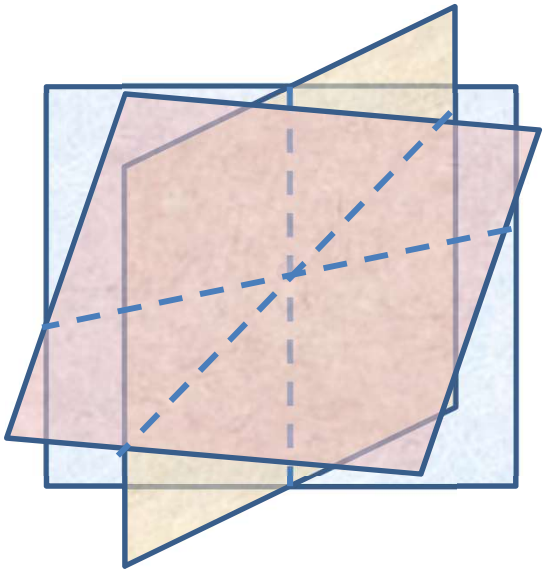

Considering the projection theorem, each FT of a projection includes the center of the Fourier space.

Two FTs of different projections share a **common line**.

Addition of a third projection allows to identify common lines between this and the previous projections…

and to determine relative **Euler angles**.

Step 2: Reconstruction

- Can we reconstruct the initial volume with an uneven angular distribution?
- How does noise affect the reconstruction?
- How to incorporate constraints?

Methods:

1) **Weighted back projection**: reconstruction of the volume in real space, using a function that inverts the projection.

However, the sampling in Fourier space is not homogeneous: high frequencies are less sampled than low frequencies, causing reduction of resolution.

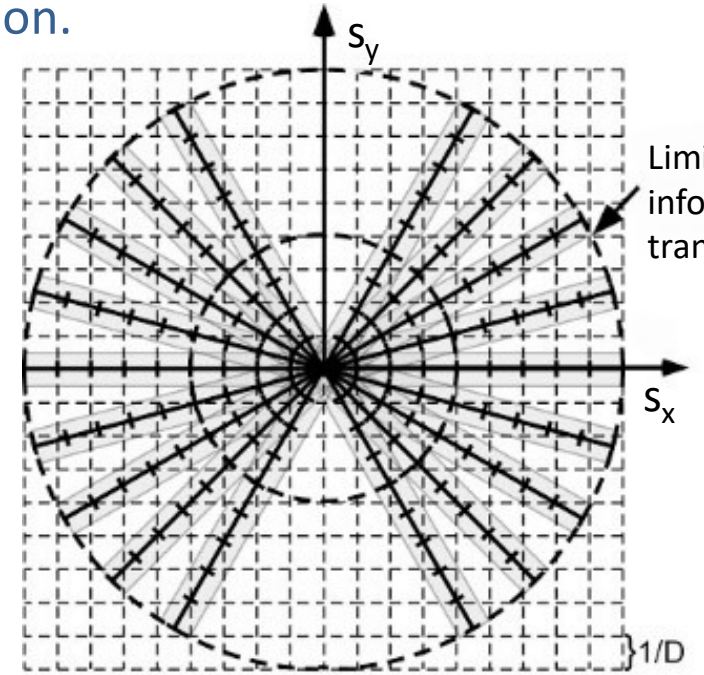

Weights applied to images before reconstruction to restore high resolution information

$$W(s) = \begin{cases} \frac{1}{H(s)} \; for \; H(s) \geq T \\ \frac{1}{T} \; for \; H(s) < T \end{cases}$$

2) **Fourier reconstruction methods**: reconstruction in reciprocal space, from the Fourier transforms of each image aligned by Euler angles

Interpolation problem due to non-homogeneous sampling of the reciprocal space.

This method is computationally intense

3) **Simultaneous Iterative Algebraic Reconstruction Method (SIRT)**: reconstruction in reciprocal space, from the Fourier transforms of each image aligned by Euler angles

For each pixel $p_j^{(i)}$ of the i-th projection

$$p_j^{(i)} = \sum_k w_{kj}^{(i)} p_k$$

p_k = each voxel of the object

$w_{kj}^{(i)}$ = weight reflecting orientation of the i-th projection and contribution of the object voxels to the projection

Iterative inversion of the matrix to obtain p_k, computing at each step distances between the experimental projections and the computed projections

CTF correction

CTF correction can be applied:

- On single raw images or micrographs, but this approach is limited due to SNR of single images
- Application of CTF correction after reconstruction, by dividing particles into defocus groups based on original micrographs. (But defocus groups should have a small step to avoid errors in CTF correction that would decrease resolution.)
- Simultaneous CTF correction and reconstruction, using iterative methods… see next slides (Relion, Freealign…)

* For Random Conic Tilt approach, additional problem due to different defocus of particles in 45°-tilted micrographs (according to position of the particle in the micrograph…)

Heterogeneity

Is it possible to separate images from different conformations of the protein/complex in the sample?

3D Classification & Refinement (RELION)

Classification based on a 3D model:

previous structure obtained from X-ray crystallography, Negative Staining EM, ab initio cryo-EM reconstruction

Iterative refinement:

use model of the previous cycle to estimate Euler angles (and CTF and/or Class assignment),
reconstruct model using back projection,
until changes are negligible

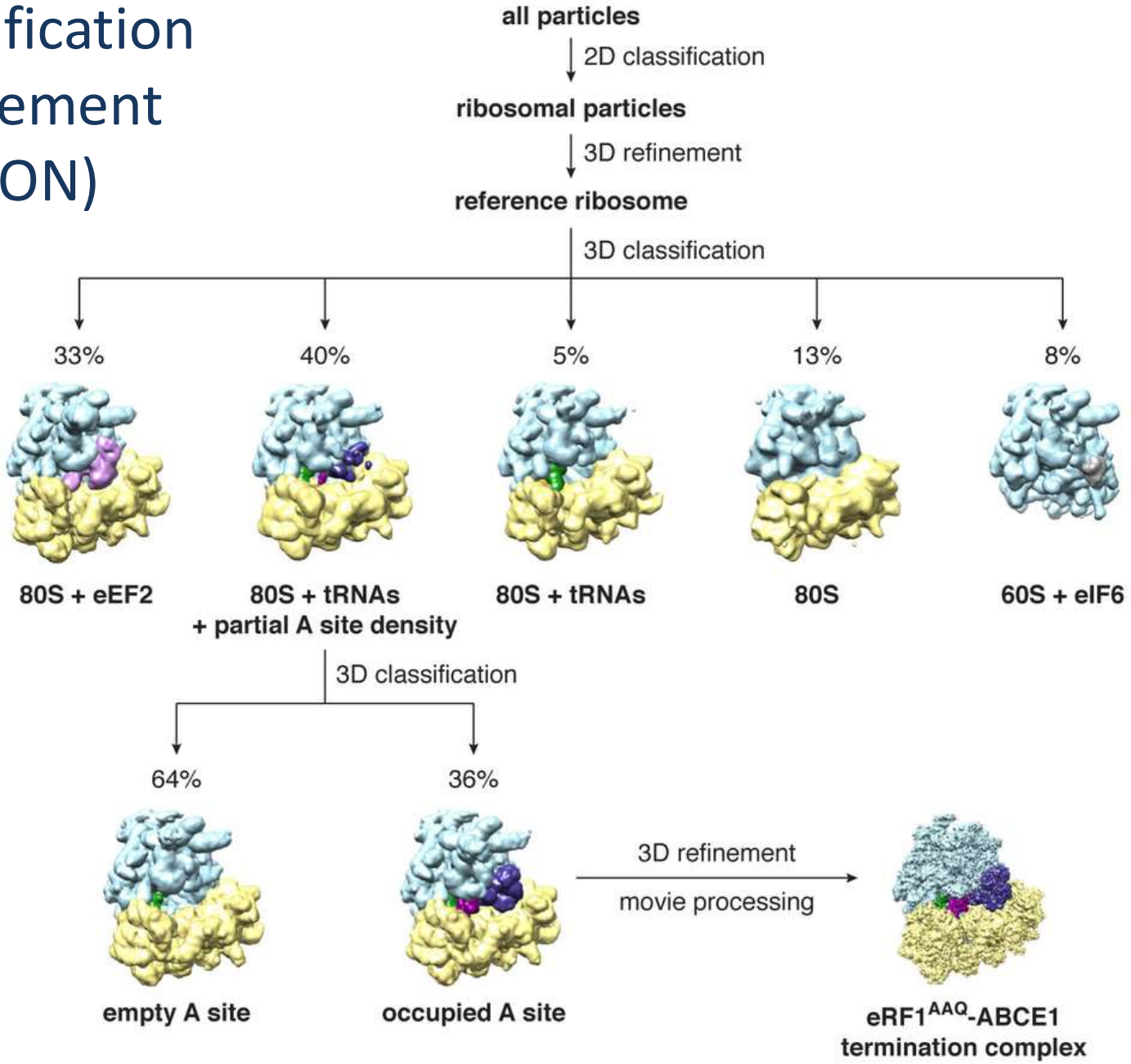

Statistical approach

Fourier space

FT(img)
X_i

+CTF$_i$
+noise N$_i$

Noise:
independent,
zero-mean,
Gaussian distributed
with variance σ_{ij}^2

Rotationally
symmetrical, but
'colored'
(frequency-
dependent):
$\sigma_i^2(\upsilon)$

back-projection ⇩

orientation, ϕ

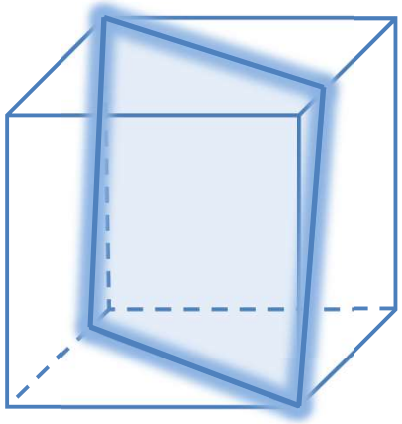

FT(object)
V_k

Probability distribution of
orientations ϕ:

$$\Gamma_{i\phi} \propto P(X_i \mid \phi, \Theta, Y)\, P(\phi \mid \Theta, Y)$$

Gaussian probability
distribution
with variance equal
to the variance of
noise σ_{ij}^2

all orientations
with equal
probability

Relion algorithm

Real space

Fourier space

image
X_i
+CTF$_i$
+noise
N$_i$

FT

FT(img)
X_i

$$X_{ij} = \sum_l \mathbf{P}_{jl}^{\phi} V_{kl}$$

+CTF$_i$
+noise N$_i$

projection

back-projection

orientation, ϕ

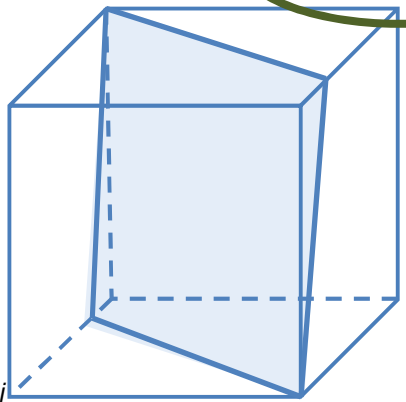

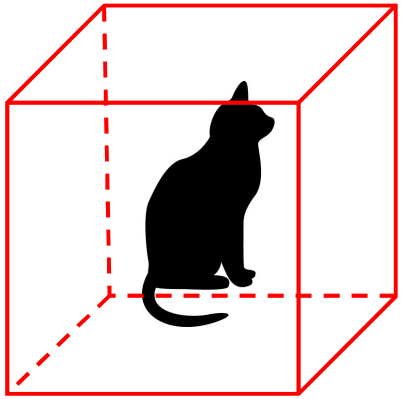

object
V_k

FT^{-1}

FT(object)
V_k

$$V_l = \sum_i \sum_j \mathbf{P}_{jl}^{\phi T} X_{ij}$$

+CTF$_i$
+Wiener filter

Iterative algorithm

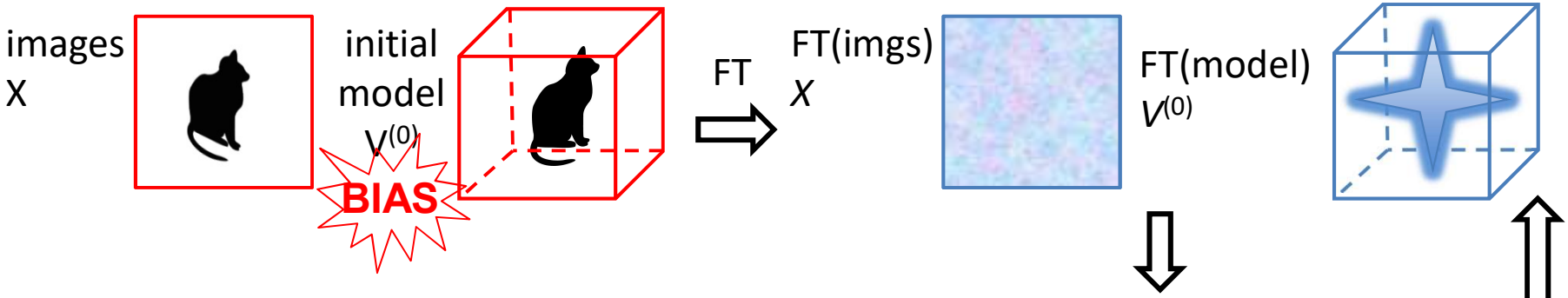

$$\Gamma_{i\phi}^{(1)} \propto \prod_j \frac{1}{2\pi\sigma_{ij}^2} \exp\left(\frac{\left| X_{ij} - CTF_{ij} \sum_l \mathbf{P}_{jl}^{\phi} V_l^0 \right|^2}{-2\sigma_{ij}^2} \right)$$

$$V_l^{(1)} \propto \sum_l \left\{ \int_\phi \left[\Gamma_{i\phi} \cdot \left(\sum_j \mathbf{P}_{jl}^{\phi T} X_{ij} \right) \right] d\phi \right\}$$

$$\sigma_{ij}^{2(1)} = \frac{1}{2} \int_\phi \Gamma_{i\phi}^{(1)} \cdot \left| X_{ij} - CTF_{ij} \left(\sum_l \mathbf{P}_{jl}^{\phi} V_{kl} \right) \right|^2 d\phi$$

$$\tau_l^{2(1)} = \frac{1}{2} \left| V_l^{(1)} \right|^2$$

Calculate:

- Probability distribution of orientations, $\Gamma_{i\phi}^{(1)}$, by comparing FT of images with slices of the Fourier space, weighted by the noise of each image.
- The new model, $V^{(1)}$, by back-projecting each image, with orientations weighted by their probability (and with an additional Weiner filter).
- The variance of the noise, $\sigma_{ij}^{2(1)}$, and the variance of the signal, $\tau_l^{2(1)}$ (used in the Weiner filter).

Iterative algorithm

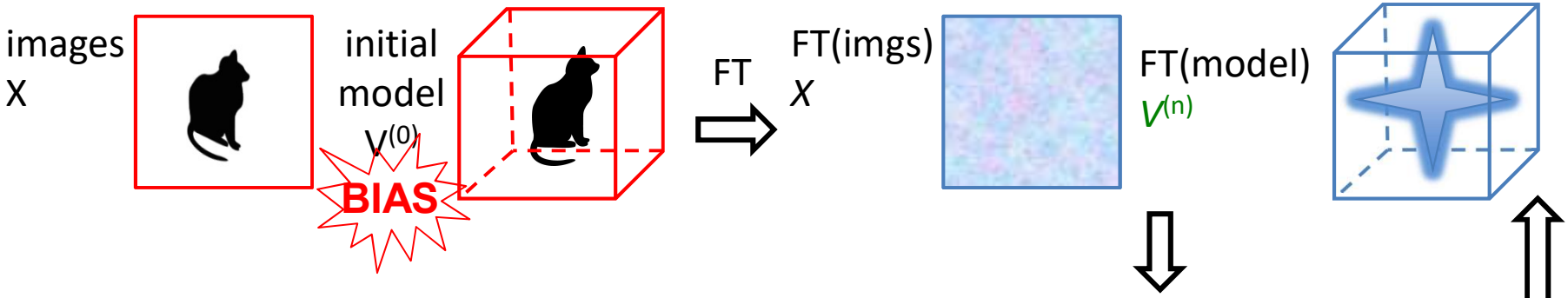

$$\Gamma_{i\phi}^{(n+1)} \propto \prod_j \frac{1}{2\pi\sigma_{ij}^{2(n)}} \exp\left(\frac{\left| X_{ij} - CTF_{ij} \sum_l \mathbf{P}_{jl}^{\phi} V_l^{(n)} \right|^2}{-2\sigma_{ij}^{2(n)}} \right)$$

$$V_l^{(n+1)} \propto \sum_l \left\{ \int_\phi \left[\Gamma_{i\phi}^{(n)} \cdot \left(\sum_j \mathbf{P}_{jl}^{\phi T} X_{ij} \right) \right] d\phi \right\}$$

$$\sigma_{ij}^{2(n+1)} = \frac{1}{2} \int_\phi \Gamma_{i\phi}^{(n)} \cdot \left| X_{ij} - CTF_{ij} \left(\sum_l \mathbf{P}_{jl}^{\phi} V_{kl}^{(n)} \right) \right|^2 d\phi$$

$$\tau_l^{2(n+1)} = \frac{1}{2} \left| V_l^{(n)} \right|^2$$

Calculate:

- Probability distribution of orientations, $\Gamma_{i\phi}^{(n+1)}$, by comparing FT of images with slices of the Fourier space, weighted by the noise of each image.
- The new model, $V^{(n+1)}$, by back-projecting each image, with orientations weighted by their probability (and with an additional Weiner filter).
- The variance of the noise, $\sigma_{ij}^{2(n+1)}$, and the variance of the signal, $\tau_l^{2(n+1)}$ (used in the Weiner filter).

Iterative algorithm

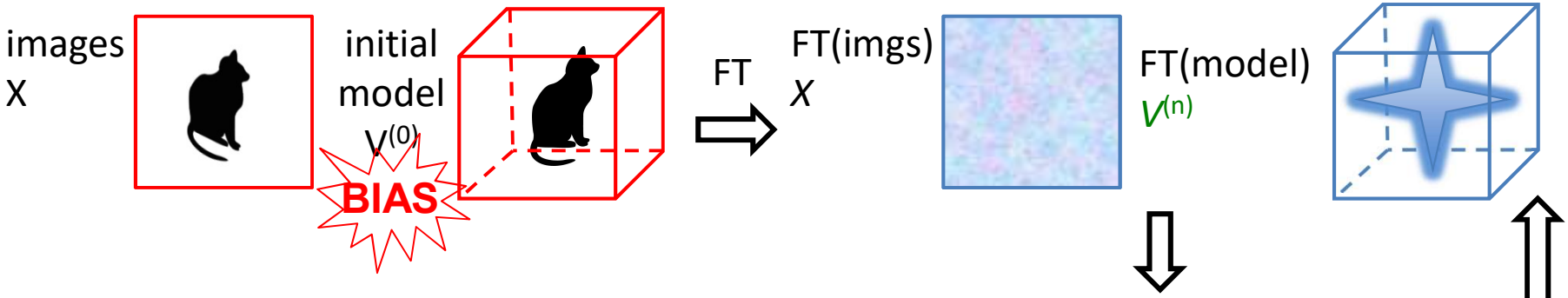

$$\Gamma_{ik\phi}^{(n+1)} \propto \prod_j \frac{1}{2\pi\sigma_{ij}^{2(n)}} \exp\left(\frac{\left| X_{ij} - CTF_{ij} \sum_l \mathbf{P}_{jl}^{\phi} V_{kl}^{(n)} \right|^2}{-2\sigma_{ij}^{2(n)}} \right)$$

$$V_{kl}^{(n+1)} \propto \sum_l \left\{ \int_\phi \left[\Gamma_{ik\phi}^{(n)} \cdot \left(\sum_j \mathbf{P}_{jl}^{\phi T} X_{ij} \right) \right] d\phi \right\}$$

$$\sigma_{ij}^{2(n+1)} = \frac{1}{2} \sum_k \left\{ \int_\phi \Gamma_{i\phi}^{(n)} \cdot \left| X_{ij} - CTF_{ij} \left(\sum_l \mathbf{P}_{jl}^{\phi} V_{kl}^{(n)} \right) \right|^2 d\phi \right\}$$

$$\tau_{kl}^{2(n+1)} = \frac{1}{2} \left| V_{kl}^{(n)} \right|^2$$

Calculate:

- Probability distribution of orientations, $\Gamma_{i\phi}^{(n+1)}$, by comparing FT of images with slices of the Fourier space, weighted by the noise of each image.
- The new model, $\boldsymbol{V}^{(n+1)}$, by back-projecting each image, with orientations weighted by their probability (and with an additional Weiner filter).
- The variance of the noise, $\sigma_{ij}^{2(n+1)}$, and the variance of the signal, $\tau_l^{2(n+1)}$ (used in the Weiner filter).

3D classification: K different classes, calculates one volume for each class $\boldsymbol{V}_k^{(n+1)}$

Structure Validation

Sources of error in Single Particle EM structure determination:

- Particle picking from template can create **model bias** (Einstein from noise)

- **Heterogeneity** of sample can create spurious features

- For NS: artifacts of stain

- Lack of completeness (preferred orientation in NS, but also in cryo)

- **Model bias** in 3D reconstruction

- **Overfitting** (alignment of noise)

Check samples using NS-EM first, to assess homogeneity of particles

VALIDATION!!!

Check reconstruction results:

- Reconstruction with different software

- Compare with previous results (MX, NMR, MD, NS-EM, etc.)

- Ab initio reconstruction avoids model bias

- Validate with tilt pairs

Carefully assess RESOLUTION!!

Inositol trisphosphate receptor (IP_3R)

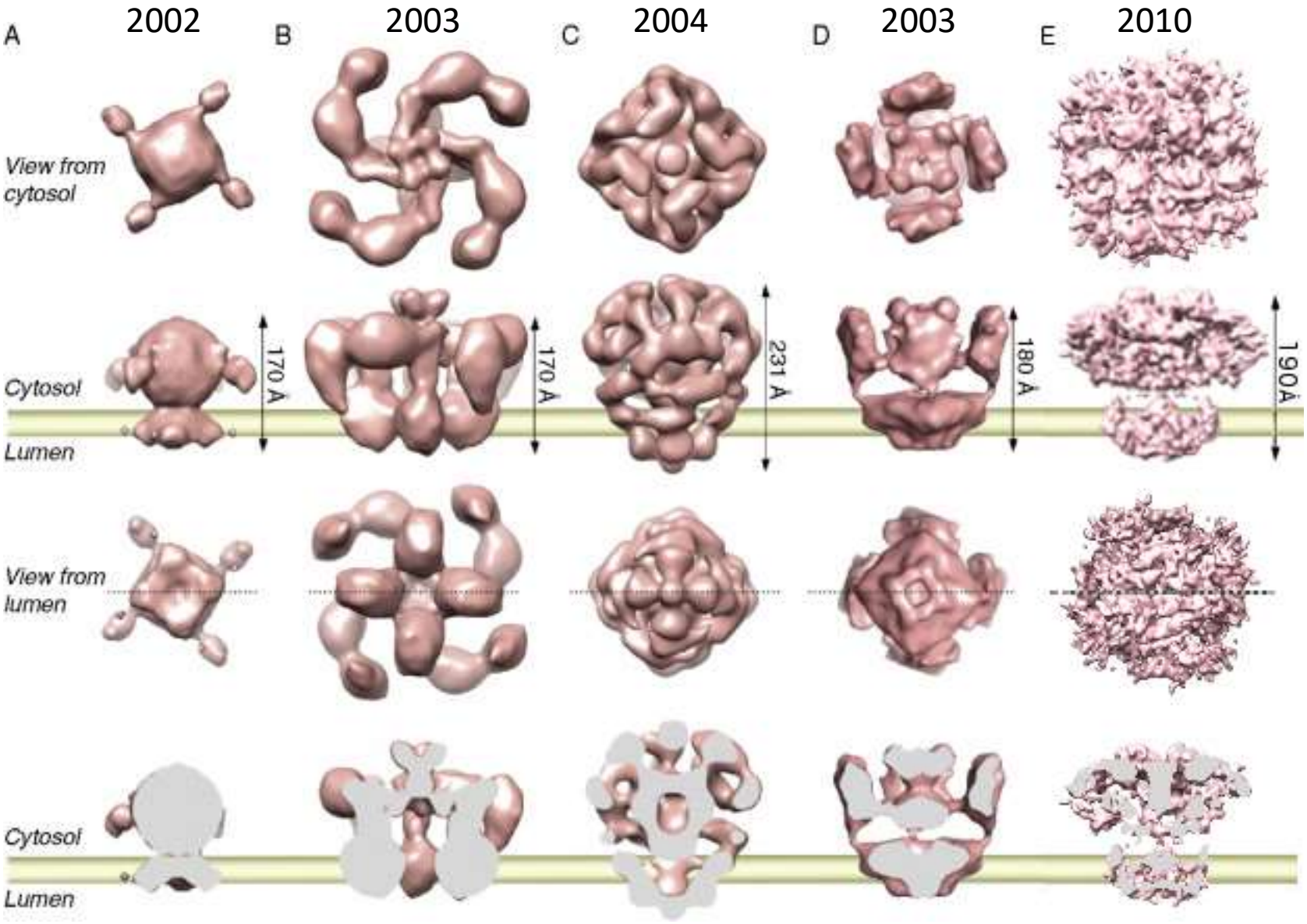

HIV-1 envelope glycoprotein

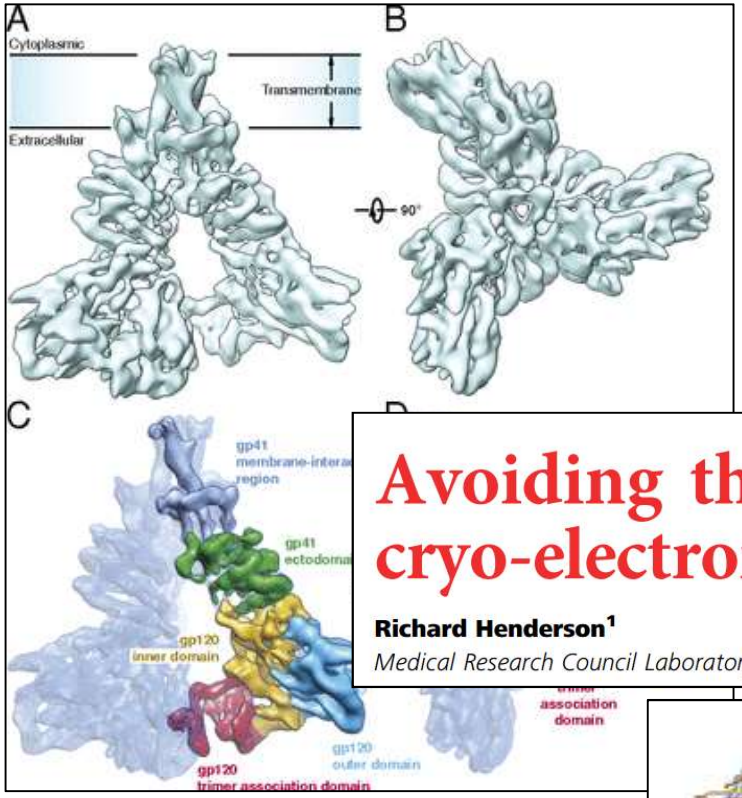

PNAS

Molecular architecture of the uncleaved HIV-1 envelope glycoprotein trimer

Youdong Mao[a,b,1], Liping Wang[a,b], Christopher Gu[a,b], Alon Herschhorn[a,b], Anik Désormeaux[c], Andrés Finzi[c], Shi-Hua Xiang[d], and Joseph G. Sodroski[a,b,e,f,1]

[a]Department of Cancer Immunology and AIDS, Dana-Farber Cancer Institute, Boston, MA 02215; [b]Department of Microbiology and Immunobiology, Harvard Medical School, Boston, MA 02115; [c]Centre de Recherche du Centre Hospitalier de l'Université de Montréal, Department of Microbiology and Immunology, Université de Montréal, Montréal, QC, Canada H3A 2B4; [d]Nebraska Center for Virology, School of Veterinary Medicine and Biomedical Sciences, University of Nebraska-Lincoln, Lincoln, NE 68583; [e]Ragon Institute of Massachusetts General Hospital, Massachusetts Institute of Technology, and Harvard, Cambridge, MA 02139; and [f]Department of Immunology and Infectious Diseases, Harvard School of Public Health, Boston, MA 02115

Avoiding the pitfalls of single particle cryo-electron microscopy: Einstein from noise

Richard Henderson[1]

Medical Research Council Laboratory of Molecular Biology, Cambridge CB2 0QH, United Kingdom

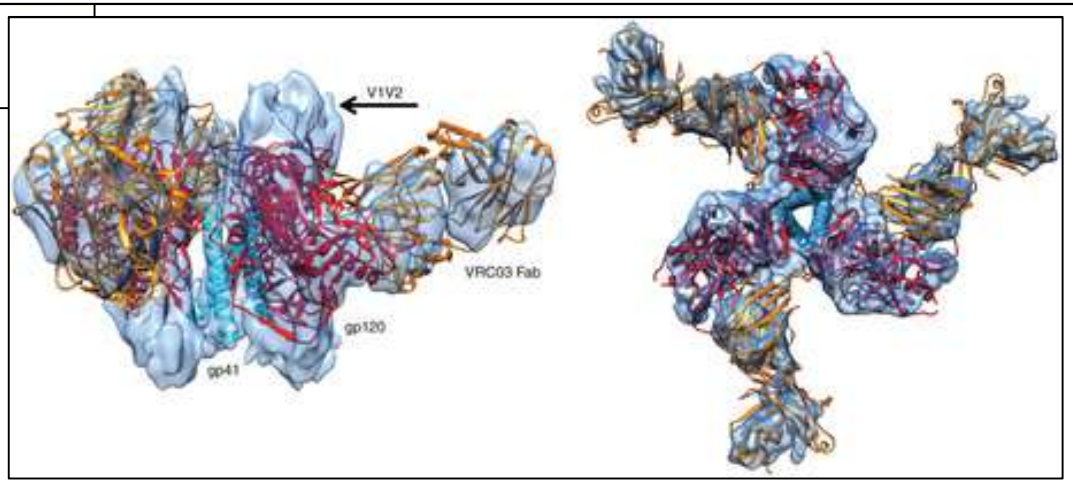

Evaluation of the quality of a structure

Determining quality of the structure is important to understand reliability of structural details

Unlike MX, no R index is available in electron microscopy to directly compare model and data.

However…

1) **Completeness** of the dataset can be evaluated by analysis of orientation frequency of particles

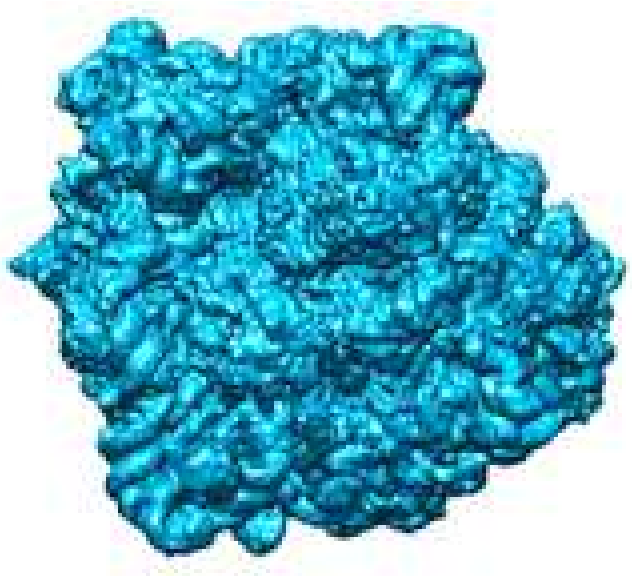

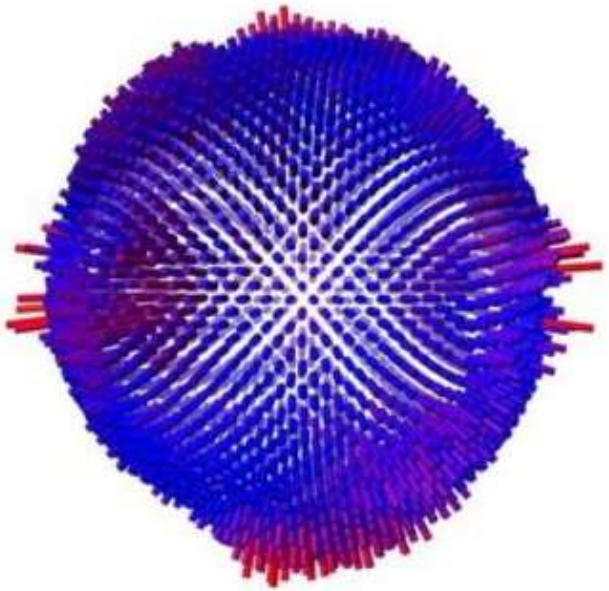

2) **Resolution**: Unlike MX, resolution has to be determined **after** data processing and structure solution

Fourier Shell Correlation (FSC)

In the Fourier space, cross correlation coefficients are calculated comparing shells of the Fourier space of the model and of the experimental data

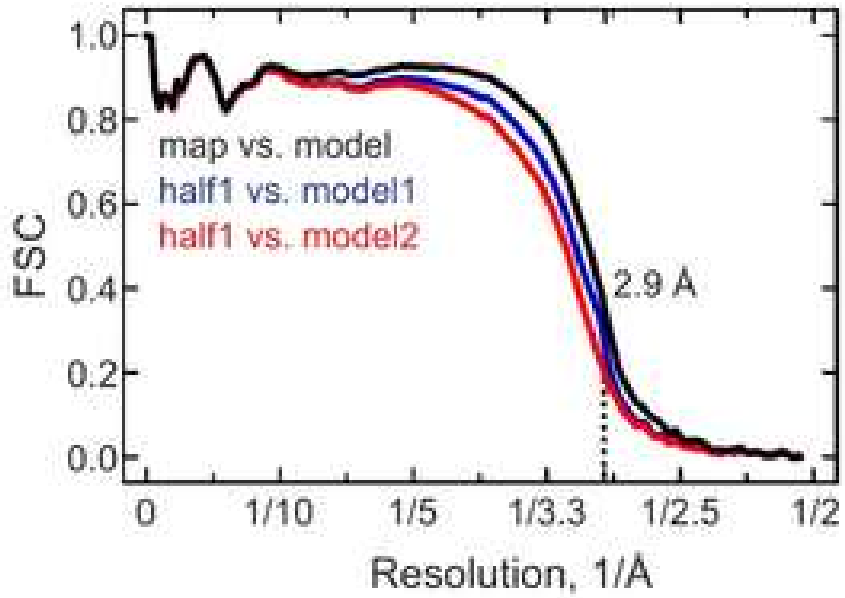

3) **Model bias?**

Fourier Shell Correlation Gold Standard: dataset is divided in 2, each half refined independently using a low-pass filtered model, FSC calculated between 2 halves

From FSC Gold Standard, resolution can be evaluated, but threshold is still a matter of debate…

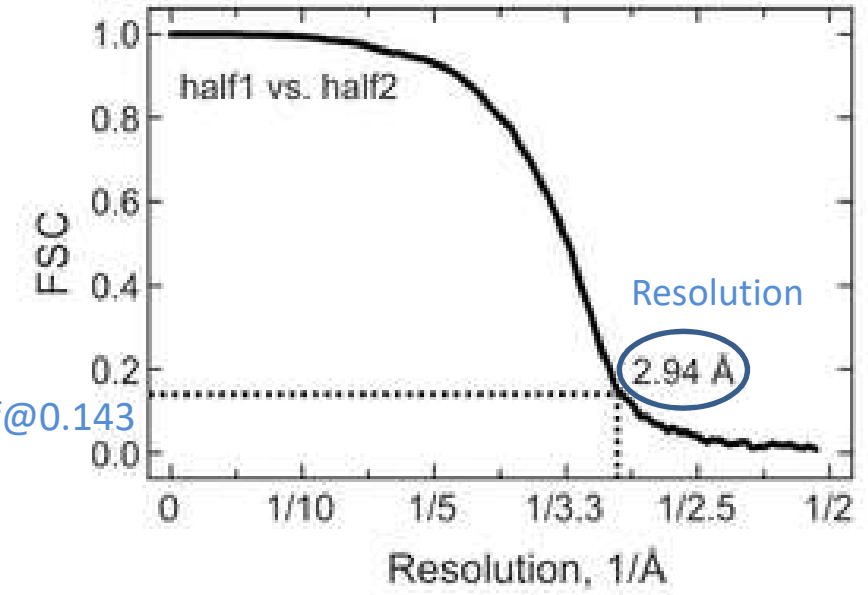

Ryanodine Receptor

Before DDD camera

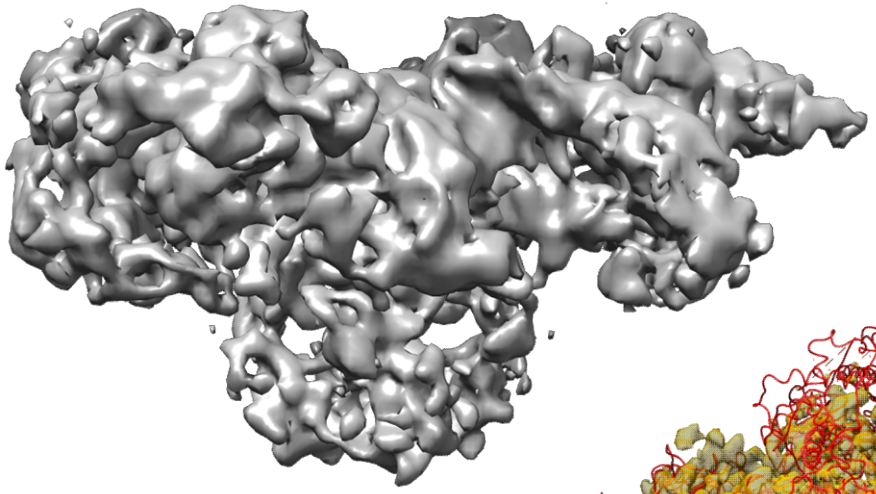

Scheres group
(MRC - Cambridge)
2015 – 3.8Å resolution

With DDD camera

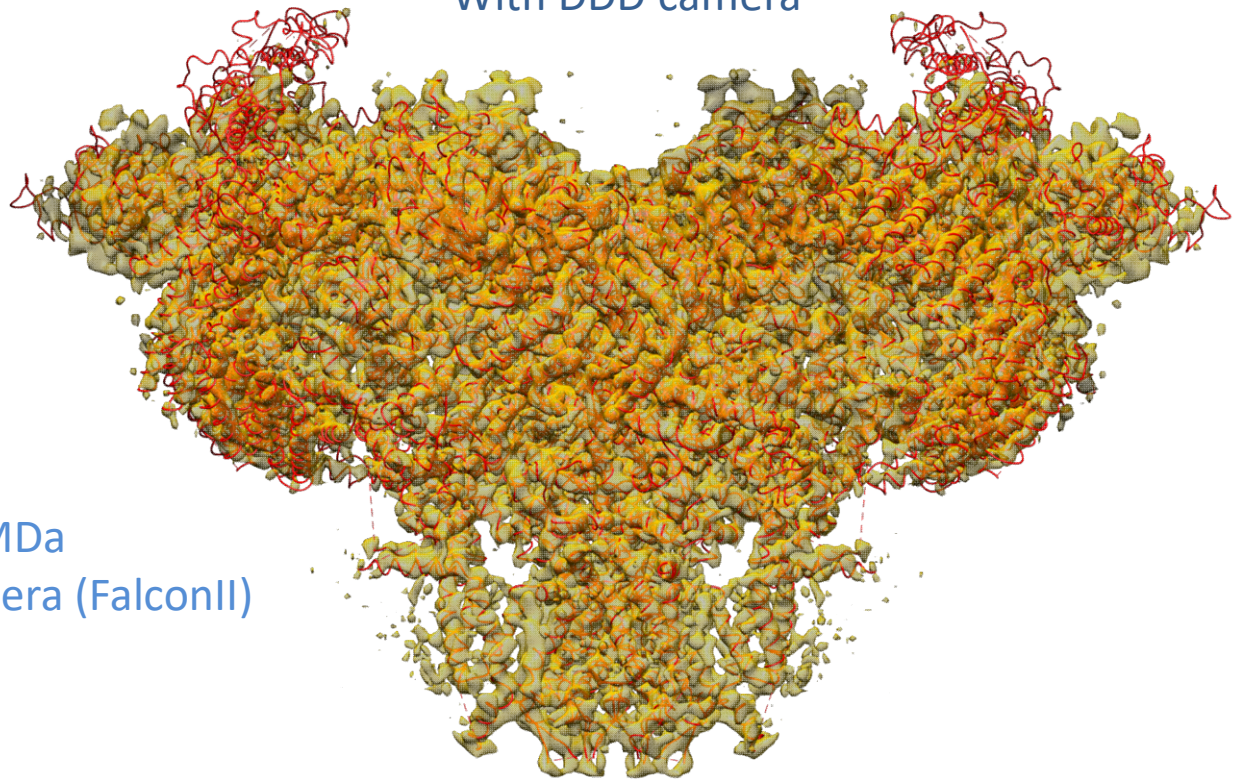

RyR
Membrane protein, 2.2MDa
Polara 300kV – DDD camera (FalconII)
3D classification Relion

Transient Receptor Potential chennel

Cheng group (UCSF)
2013 - 3.2Å resolution

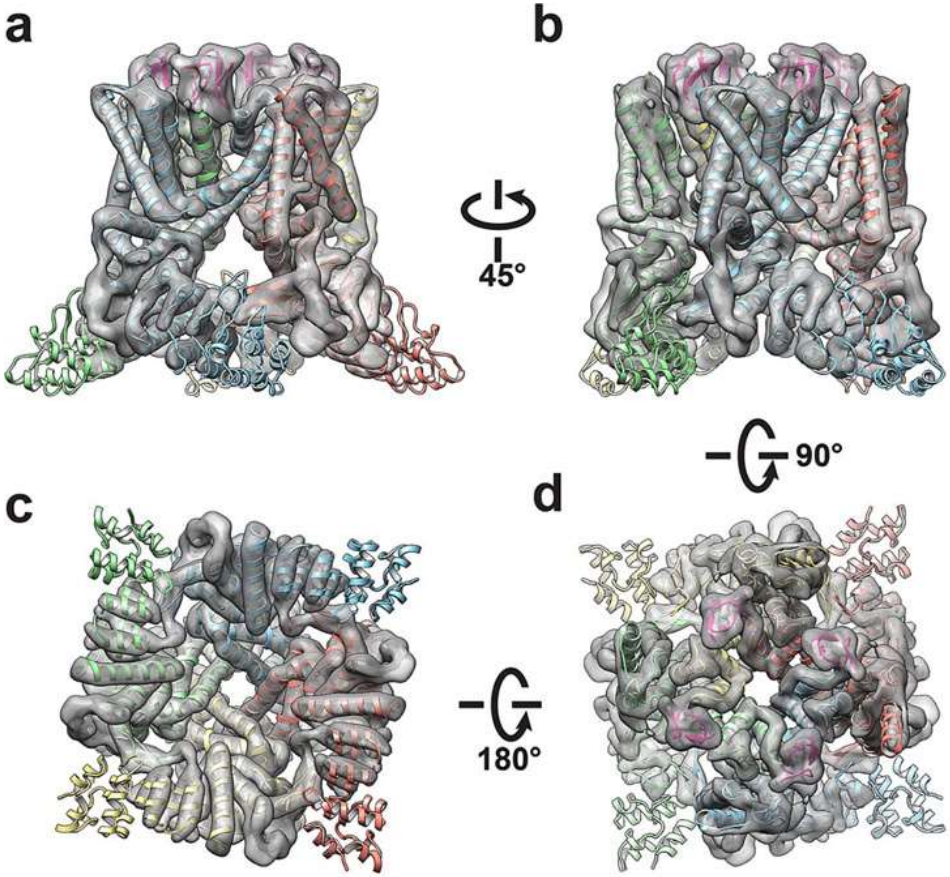

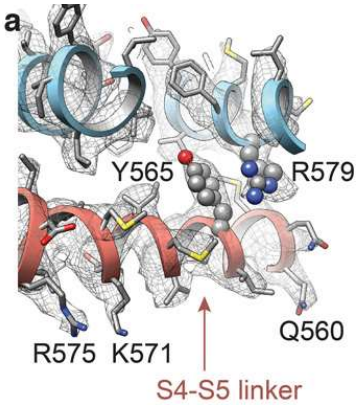

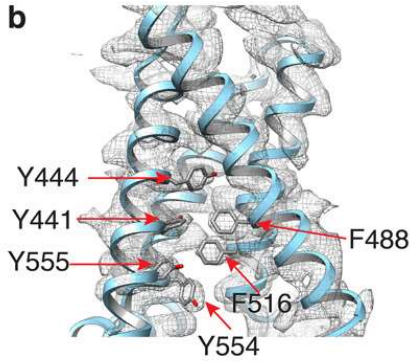

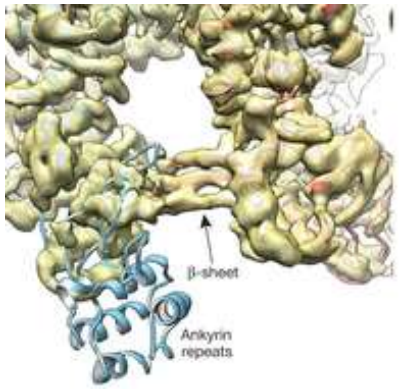

TRPV1
Membrane protein, 180kDa
Polara 300kV – DDD camera (K2)
3D classification Relion

Apoferritin

2020 - 1.22 Å resolution

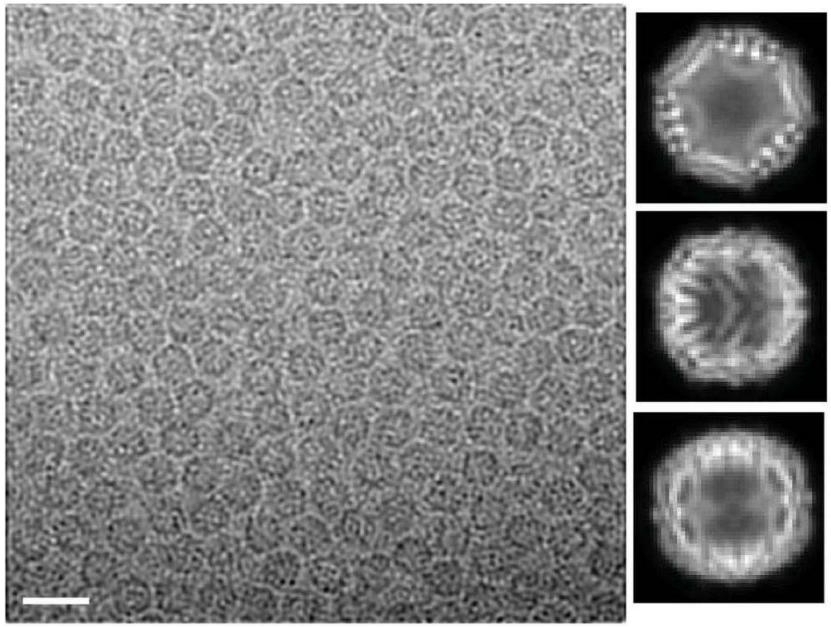

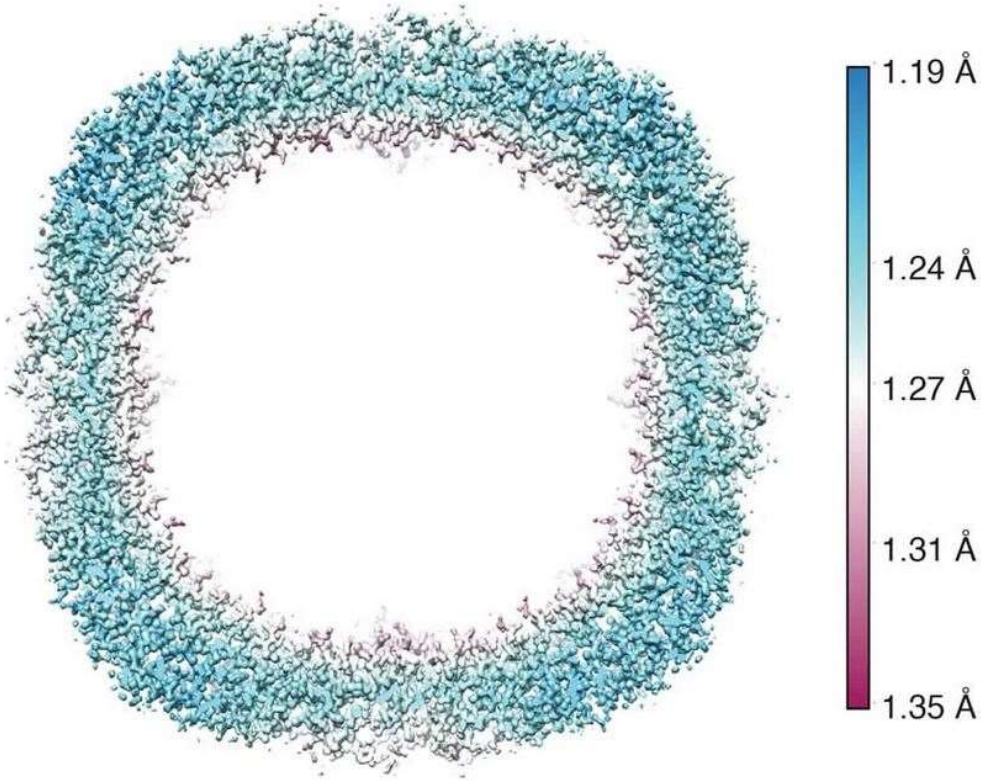

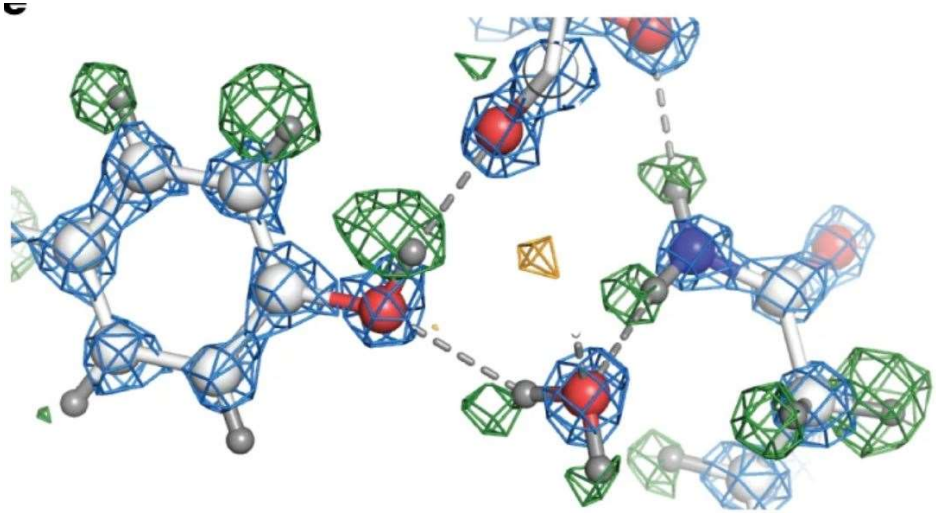

Apoferritin
Soluble protein, 24-fold symmetry, 500 kDa
Prototype Cold-FEG, 300kV
DDD camera (Falcon4) – Energy filter
3D classification: Relion
PDB: 7A4M – EMDB: EMD-11638

β-Galactosidase

Subramaniam group (NIH)
2014 - 2.2 Å resolution

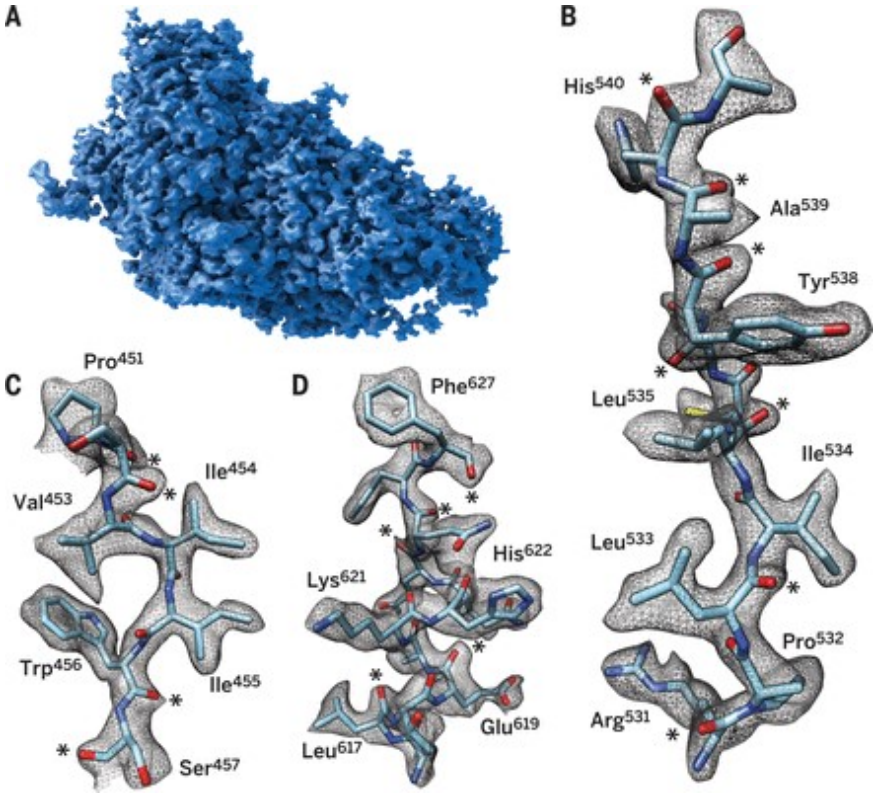

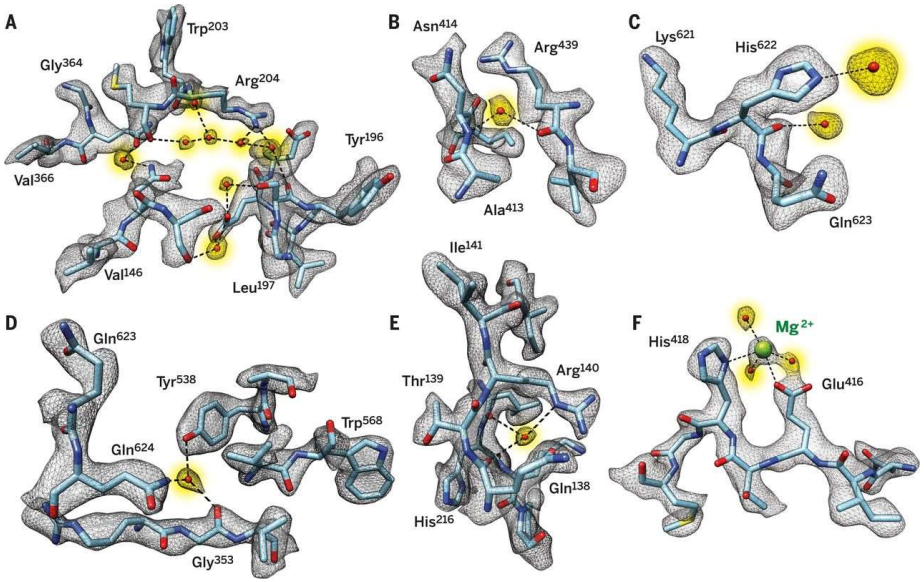

β-Galactosidase
Soluble protein, 465kDa
Titan Krios 300kV – DDD camera (K2) – Energy filter
3D classification Frealign

Microtubule structure and dynamics

A successful example of an integrative approach to a structural biology problem

1980-1990

Electron Crystal.
Sheets antiparallel protofilaments

Assembly of αβ-tubulin dimers is a spontaneous process, while disassembly requires GTP hydrolysis.

2000

X-ray Crystal.
Dimers bound to depolymerizing proteins

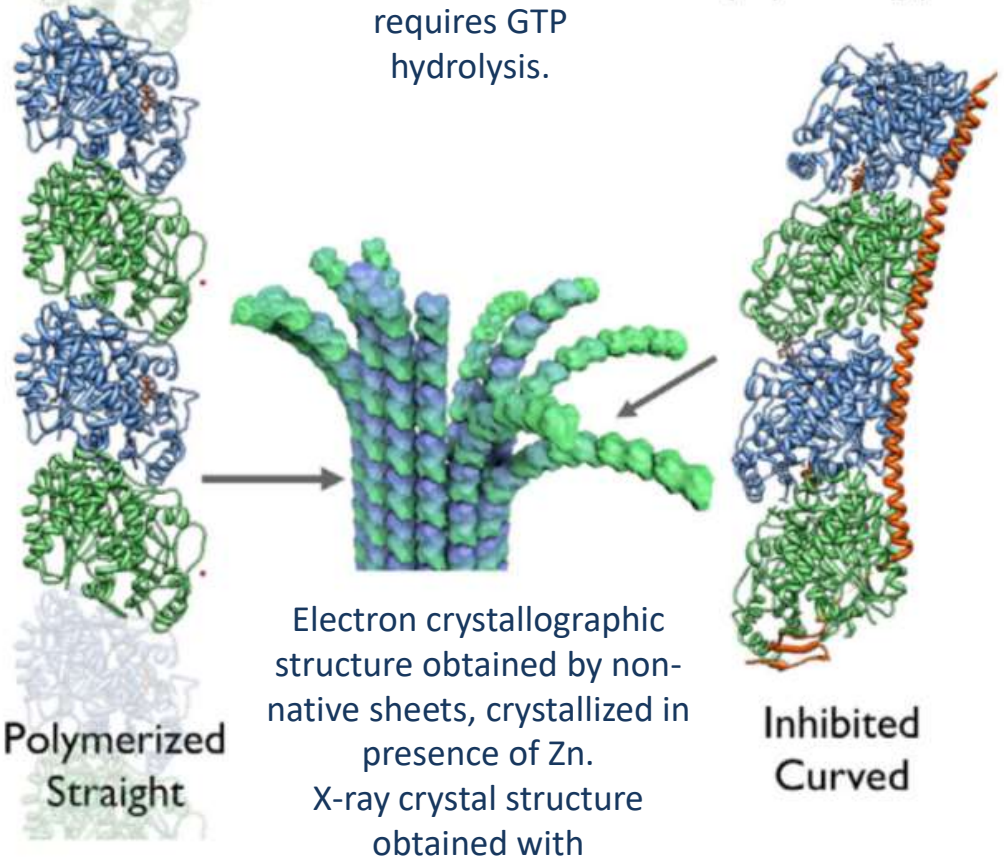

Electron crystallographic structure obtained by non-native sheets, crystallized in presence of Zn.
X-ray crystal structure obtained with depolymerizing protein.

1999-2015

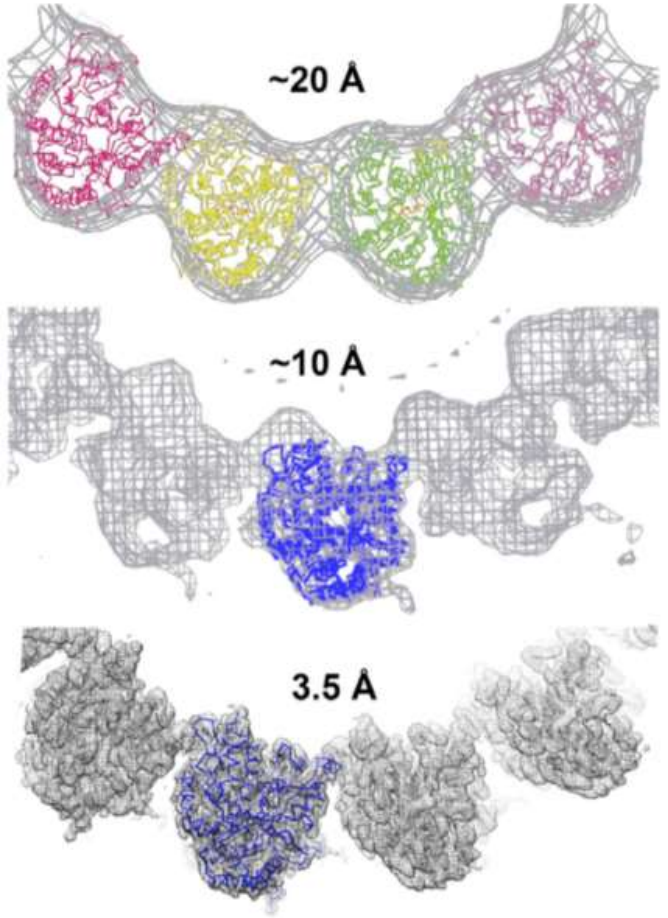

Single-particle cryo-EM

Cryo-EM studies on *in vitro* reconstituted microtubules with native conformation.

Dynein walk

Cryo-EM and X-ray structures of microtubule-dynein complexes allowed to understand mechanism of «dynein walk» on microtubule

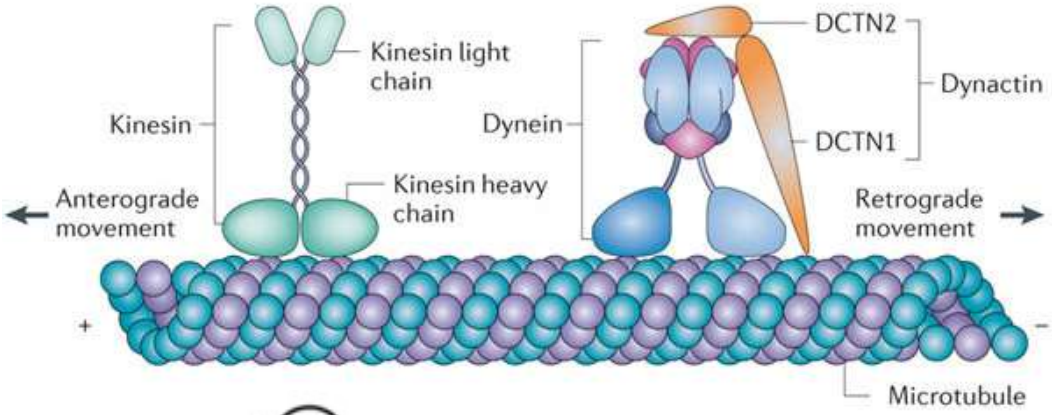

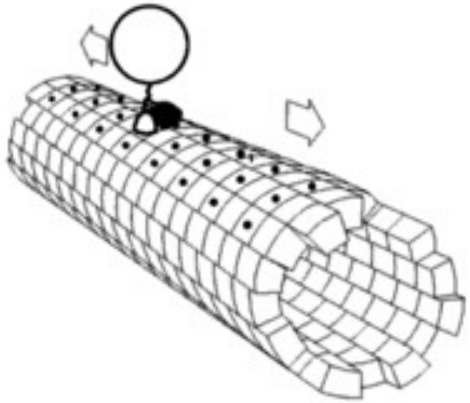

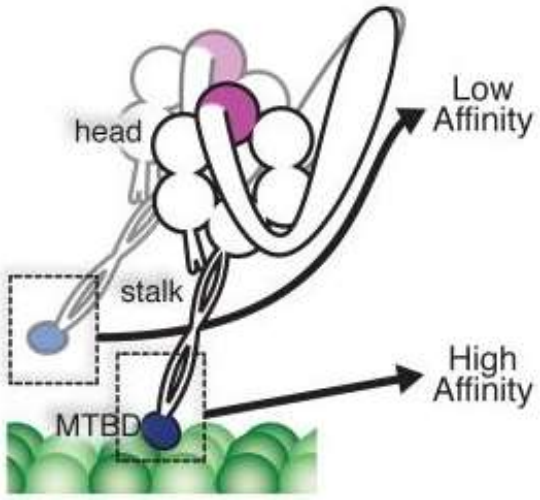

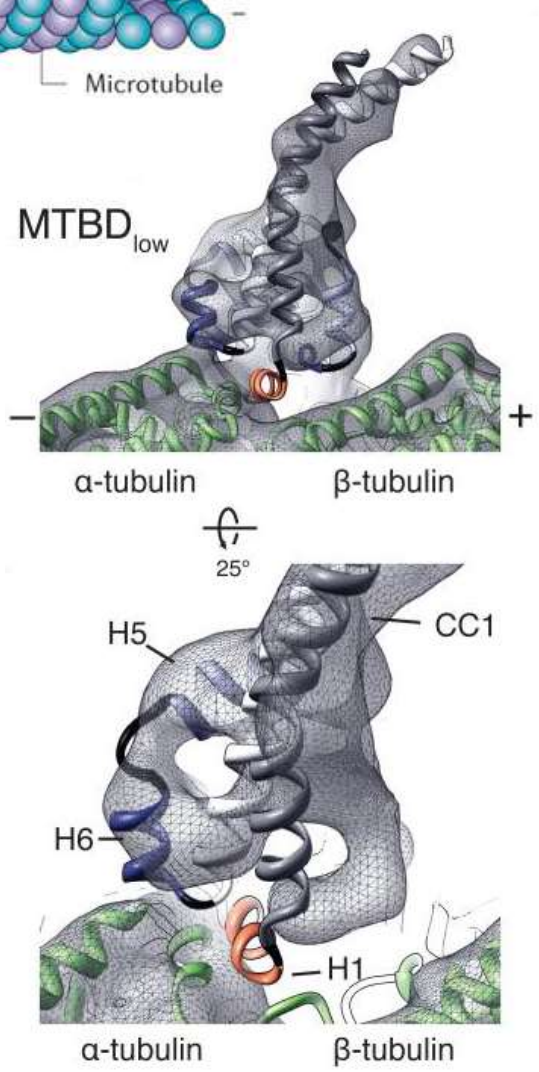

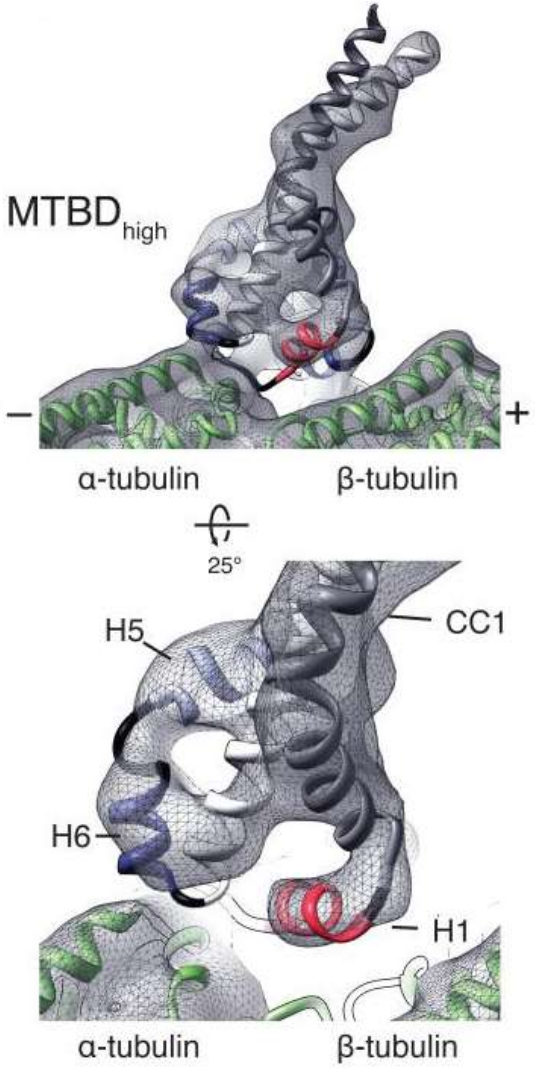

References

- Single-particle electron microscopy: Cheng Y. *et al.*, "A primer to single-particle cryo-electron microscopy.", **Cell. 2015**, *161(3)*:438-49; De Zorzi R. *et al.*, "Single-particle electron microscopy in the study of membrane protein structure.", **Microscopy (Oxf). 2016**, *65(1)*:81-96.
- Relion algorithm: Scheres S.H., "RELION: implementation of a Bayesian approach to cryo-EM structure determination.", **J Struct Biol. 2012**, *180(3)*:519-30; Scheres S.H., "A Bayesian view on cryo-EM structure determination.", **J Mol Biol. 2012**, *415(2)*:406-18.
- Cautionary tales: Henderson R., "Avoiding the pitfalls of single particle cryo-electron microscopy: Einstein from noise.", **Proc Natl Acad Sci U S A. 2013**, *110(45)*:18037-41; Fan G. *et al.*, "Gating machinery of $InsP_3R$ channels revealed by electron cryomicroscopy.", **Nature. 2015**, *527(7578)*:336-41.
- Ryanodine receptor: Cheng Y. *et al.*, "A primer to single-particle cryo-electron microscopy.", **Cell. 2015**, *161(3)*:438-49; De Zorzi R. *et al.*, "Single-particle electron microscopy in the study of membrane protein structure.", **Microscopy (Oxf). 2016**, *65(1)*:81-96.
- TRPV1 channel: Liao M. *et al.*, "Single particle electron cryo-microscopy of a mammalian ion channel.", **Curr Opin Struct Biol. 2014**, *27*:1-7; Liao M. *et al.*, "Structure of the TRPV1 ion channel determined by electron cryo-microscopy.", **Nature. 2013**, *504(7478)*:107-12; Cao E. *et al.*, "TRPV1 structures in distinct conformations reveal activation mechanisms.", **Nature. 2013**, *504(7478)*:113-18.
- β-Galactosidase: Bartesaghi A. *et al.*, "2.2 Å resolution cryo-EM structure of β-galactosidase in complex with a cell-permeant inhibitor.", **Science. 2015**, *348(6239)*:1147-51.
- Microtubule: Nogales E., "An electron microscopy journey in the study of microtubule structure and dynamics.", **Protein Sci. 2015**, *24(12)*:1912-9; Redwine W.B. *et al.*, "Structural basis for microtubule binding and release by dynein.", **Science. 2012**, 337(6101):1532-6.
- Apoferritin: Nakane T. *et al.*, "Single-particle cryo-EM at atomic resolution.", **Nature. 2020**, *587*:152-6.